Gas Sensing Application of Ceria, Cassiterite and Ceria-Cassiterite Nanocomposite

Mane C.B.[2], Pawar R.P.[3], Tapase A.S.[4], More H.S.[5], Jadhav B.V.[6] and Patil R.P.[1*]
1. Department of Chemistry, M.H. Shinde Mahavidyalaya, Tisangi 416206, MH, INDIA
2. Department of Chemistry, Shri Vijaysinha Yadav College of Arts and Science, Peth Vadgaon, MH, INDIA
3. Government Vidarbha Institute of Science and Humanities, VMV Road, Amravati, 444 604 MH, INDIA
4. Department of Chemistry, Dattajirao Kadam Arts, Science and Commerce College, Ichalkaranji, 416 115 MH, INDIA
5. Department of Physics, Sanjay Ghodawat University, Kolhapur-416118 MH, INDIA
6. Department of Chemistry, Changu Kana Thakur Arts, Commerce and Science College, New Panvel 400035, MH, INDIA
*patilraj_2005@rediffmail.com

Abstract
Ceria, Cassiterite and Ceria-Cassiterite nanocomposites are studied as potential candidates for gas sensors. The particles of CeO_2 core and SnO_2 shell nanocomposite were prepared by microwave method. X-ray diffraction and transmission electron microscopy were used to characterize the CeO_2, SnO_2 and CeO_2/ SnO_2 core shell nanocomposites. The obtained results from XRD show that the CeO_2 nanoparticles coated on SnO_2 yields diffraction peaks correspond to the crystalline SnO_2 phase. Also, TEM results show that the nanocomposite particles have a spherical morphology and a narrow size distribution. The thickness of CeO_2 shell on the surface of SnO_2 particles was about 7 nm. The particle size of the CeO_2 and SnO_2 and their nano composite is in the range of 10-20 nm. The electrical resistivity is decreasing with increasing temperature for all the samples. This indicates that all the samples show semiconductor like behavior.

The present work describes the gas-sensing performance of the nanostructured CeO_2, SnO_2 and CeO_2-SnO_2 powder towards ethanol, LPG, H_2, CO_2, NH_3 andCl_2. It was found that the material exhibits high selectivity and sensitivity towards 60 ppm LPG at the operating temperature of $150^{O}C$.

Keywords: Ceria, cassiterite, nanocomposite, gas sensors, PPM.

Introduction

Gas sensors based on metal dioxide and their nanocomposites have attracted much public attention during the past decades due to their excellent potential for applications in environmental pollution remediation, transportation industries, personal safety, biology and medicine[1-3].

Numerous efforts have therefore been devoted to improving the sensing performance of metal oxides. In those effects, the construct of nanoheterostructures is a promising in gas sensing modification which shows superior sensing performance to that of the single component based sensors. Since the 20th century, atmospheric pollution has been proved to be one of most urgent issues. For the sake of controlling the exhaust emissions, gas sensors for the quantitative detection of various toxic and harmful gases have been widely developed as a result of their high response, outstanding selectivity, excellent repeatability and good stability[4–6].

So far a variety of gas sensors such as metal oxide semiconductor-based gas sensors[7–12], solid electrolyte-based gas sensors[13], electrochemical gas sensors[14], carbon-based gas sensors[15–17], organic gas sensors[5,6] and so on have been extensively investigated.

Amongst these different types of gas sensors, resistance type metal oxide gas sensors offering low cost, simple manufacturing approaches and excellent sensitivity to the great majority of gases have attracted considerable attention during the past several years[18,19].

SnO_2 is a special oxide material because it has a low electrical resistance with high optical transparency in the visible range. SnO_2 owing to a wide bandgap is an insulator in its stoichiometric form. However, due to the high intrinsic defects, that is oxygen deficient SnO_2 is an n-type semiconductor and has many applications. Similarly, CeO_2 is reported to be a predominantly ionic conductor, exhibits n-type conductivity under certain conditions. Cerium dioxide is an inexpensive and relatively harmless material that presents several characteristics that could be potentially advantageous for gas sensing applications. SnO_2 and CeO_2 nanomaterials reveal that they are promising materials for optoelectronic devices such as solar cells, conductive layers and transistors.

In this study, we briefly summarize and highlight the development of CeO_2, SnO_2 and CeO_2-SnO_2 based heterostructure gas sensing materials with diverse models, including semiconductor/semiconductor nano-heterostructures, which have been investigated for effective enhancement of gas sensing properties through the increase of sensitivity, selectivity and stability.

Also, we report the synthesis, characterization and gas sensing of CeO_2, SnO_2 and CeO_2-SnO_2 novel microwave system and describe the gas-sensing performance of the nanostructured CeO_2, SnO_2 and CeO_2-SnO_2 powder towards ethanol, LPG, H_2, CO_2, NH_3 andCl_2.

Material and Methods

Ceria (CeO_2) and cassiterite (SnO_2) have been synthesized by microwave method. All the chemicals are of analytical grade. About 2.2565 g of $SnCl_4$. $2H_2O$ is dissolved in 100 ml distilled water. 30 ml of above solution is taken in 250 ml beaker and 45 ml 1M ammonia solution was added dropwise with constant stirring till precipitation completed and gel is formed. Then the solution was kept in (800 W EO-77 HORNO ELECTRICO, ORBIT) microwave oven at 353K for 30 min. The resulting gel was filtered through Whatmann filter paper no. 40, then it is dried at 353K for 24 Hrs in order to remove moisture or water molecule present in it. Then the precipitate obtained was collected in silica crucible and calcination was carried out at 773K for 2 hrs; finally, ash colored tin oxide nanoparticles were formed. Similarly, cerium oxide has been synthesized. Also, Ceria- cassiterite nanocomposite was prepared by sol–gel hydrolysis.

X-ray diffractometer (Philips model PW-1710) was used to identify the crystalline nature of the samples using CuKα radiation. Particle size was measured using a transmission electron microscope (TEM) (Philips, CM200, operating voltages 20–200 kV). Gas sensing performances of CeO_2, SnO_2 and CeO_2-SnO_2 metal oxides and nanocomposities were tested against various oxidizing and reducing gases.

Characterization Techniques: The phase formation of the sintered samples was confirmed by X-ray diffraction studies using Philips PW-1710 X-ray diffractometer with CuKα radiation (λ=1.54178Å). The lattice parameters were calculated for the cubic phase using following relation.

For cubic phase $$a = d\,(h^2+ k^2 +l^2)^{1/2} \quad (1)$$

where a = Lattice parameters, (hkl) = Miller indices and d = interplanar distance.

Transmission electron microscope (Philips CM 20) was used to evaluate the nanostructure of the typical samples. Two probe techniques were employed to measure the D.C. resistivity of the samples in the temperature range of room temperature to 723 K.

Gas sensing performances of metal oxides were tested against various oxidizing and reducing gases. The electrical resistance of a sensor in dry air is measured by Keithley Autoranging Picoammeter - Cleveland OH with use of conventional circuitry in which the sensor is connected to an external resistor at circuit voltage of 10 V (Aplab 7212 regulated power supplier). The values of device resistor are obtained by monitoring the output voltage across the load resistor. The resistance of the sensor was measured in the presence and absence of the test gas.

A known amount of gas was introduced to attain the required level of its concentration. The gas sensing measurements were carried out at different operating temperatures (373 – 623 K). The gas response (S) is defined as the ratio of ΔR i.e. the change in resistance of the sensor in air (R_a) and in presence of gas (R_g), normalized to the value of sensor resistance in air.

$$(\%)\ S = \left| R_a - R_g \right| / R_a \,x100 \quad (2)$$

Results and Discussion

XRD studies: X-ray diffraction patterns of the Ceria (CeO_2) cassiterite (SnO_2) and Ceria-cassiterite samples are shown in fig. 1. A definite line broadening of the diffraction peaks indicated that the prepared single phase and multiphase metal oxides are in the nanometer range. The diffraction pattern of SnO_2 shows peaks corresponding to planes (111) (101) (200) (211) (002) (310) (301) (202) and (321) confirming the formation of SnO_2 (JCPDS Patterns No.41-1445). Diffraction peaks corresponding to planes (111) (200) (220) and (311) of CeO_2 (JCPDS Patterns No.75-076) besides that of SnO_2 are seen in the CeO_2 coated samples indicating the biphasic nature of the samples. From the X-ray, diffraction peaks average particle size was estimated using Scherrer's formula.

$$t=0.9\lambda/\beta \cos\theta \quad (3)$$

where 0.9 is the Scherrer's constant (k), **λ** is the X-ray wavelength corresponding to CuKα, β denotes the full-width at half-maximum of the peak and θ is the Bragg angle. The crystallite size was found to be in the range of 25-30 nm. The X-ray density (dx) was calculated using the relation.

$$dx = 8\ M / N\ a^3 \quad (4)$$

where N=Avagadros number ($6.023x10^{23}$atom/mole). The values of lattice constant (a), x-ray density (dx) and crystallite size are summarized in table 1.

TEM analysis: Fig. 2 depicts the transmission electron micrograph of CeO_2, SnO_2 and CeO_2-SnO_2 nanocomposite samples. It is evident that the average particle size of CeO_2 and SnO_2 is around 10-15 nm. Fig. 2 clearly shows the presence of a dispersed phase of CeO_2 on SnO_2.

Table 1
Data on lattice parameter, crystallite size, x-ray density of CeO_2 and SnO_2 samples.

Composition (x)	Lattice parameter Å	Crystallite Size (t) (nm)	X-ray density, (dx) (g/cm³)
CeO_2	5.406	35	3.513
SnO_2	4.748	22	3.025

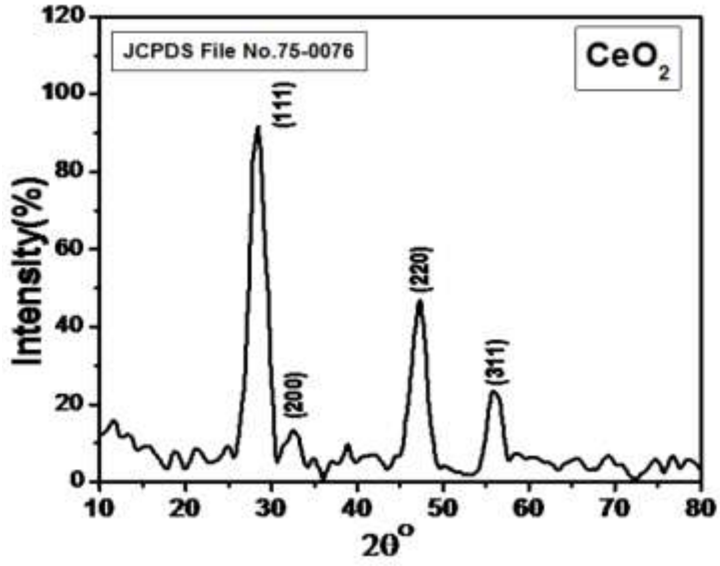

(a)

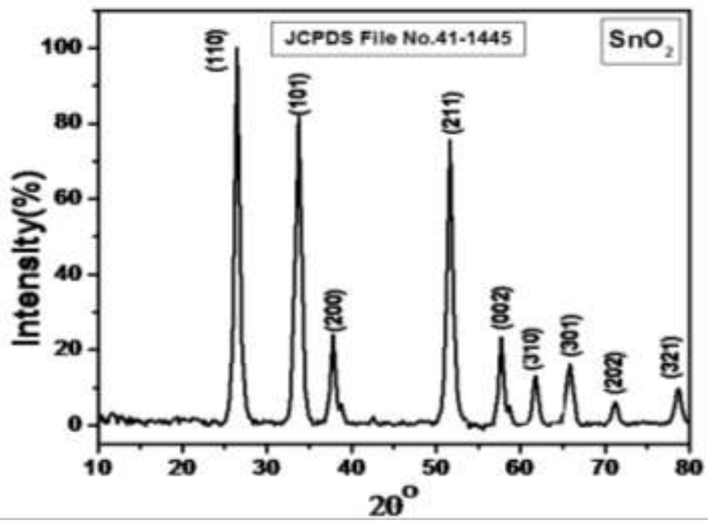

(b)

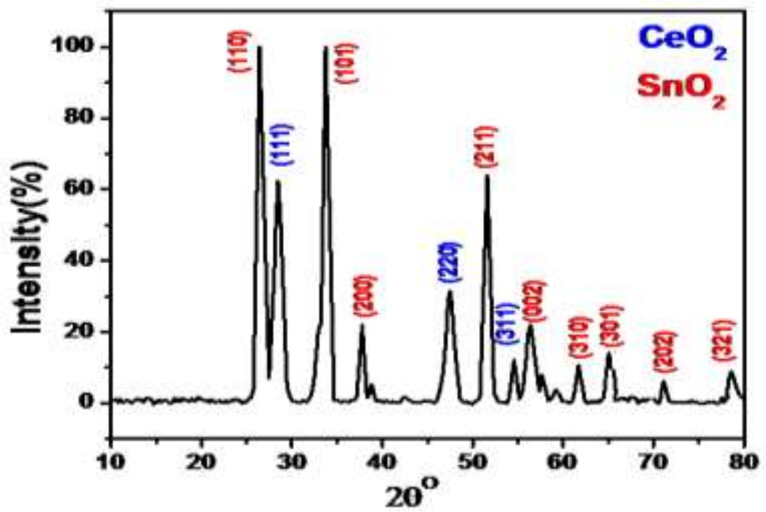

(c)

Fig. 1: XRD Patterns of (a) CeO_2 (b) SnO_2 and CeO_2-SnO_2

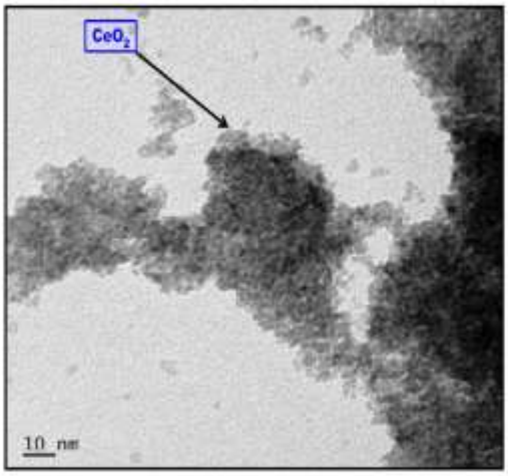

(a)

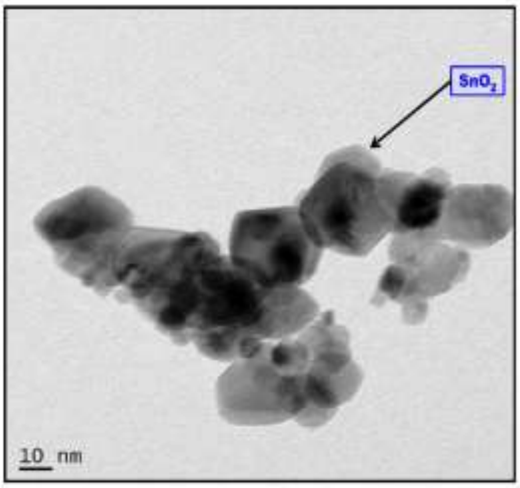

(b)

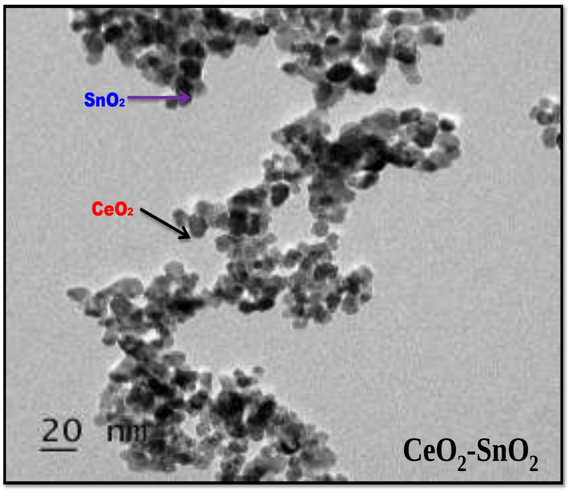

(c)

Fig. 2: TEM Image of (a) CeO_2 (b) SnO_2 and (c) CeO_2-SnO_2

Electrical Resistivity: Temperature dependence of resistivity (ρ) of samples sintered at 973K for 8h was studied over the temperature range from room temperature to 623K and they are shown in fig. 3. It can be seen that the resistivity decreases with increasing temperature for all samples. The observed behavior clearly indicates that the present CeO_2, SnO_2 and CeO_2-SnO_2 samples have semiconductor-like behavior. The resistivity arises due to the mobility of the extra electron, which comes from the crystal lattice. The movement is described by a hopping mechanism, in which the charge carriers jump from one ionic site to the next. The decrease of the electrical resistivity with increasing temperature may be related to the increase of the drift mobility of thermally activated charge carriers (electron and hole) according to hopping conduction mechanism.

Gas sensing study: Fig.4 shows gas sensing performance of each composition of the CeO_2, SnO_2 and CeO_2-SnO_2 system has been tested for various oxidizing and reducing gases viz. ethanol, LPG, H_2, Cl_2 CO_2 and ammonia gas. To investigate gas-sensing properties, the crystalline nanosized powder in the form of pellets was used. The pellets of diameter 8 mm and thickness 2 mm were made under pressure of 5 tons/cm^2 using hydraulic press followed by sintering at 400 ^{0}C for 2 h. These pellets were then subjected for studying their sensitivity and selectivity at different controlled temperatures towards various gases in the dynamic setup. It is seen from the figure that the gas sensing study shows that CeO_2 has selective response for LPG at 150°C.

The gas sensing mechanism for metal oxides in LPG can be explained as follows. It is well known that LPG contains CH_4, C_3H_8 and C_4H_{10} etc. In these substrates, reducing hydrogen species are bound to the carbon atom.

Therefore, the LPG dissociates very slowly into the reactive reducing components on the surface of the sensor. When the nanosized metal oxides are exposed to the reducing gases like LPG, they react with chemisorbed oxygen thereby releasing an electron back to conduction bands which decreases the resistance of the sensor.

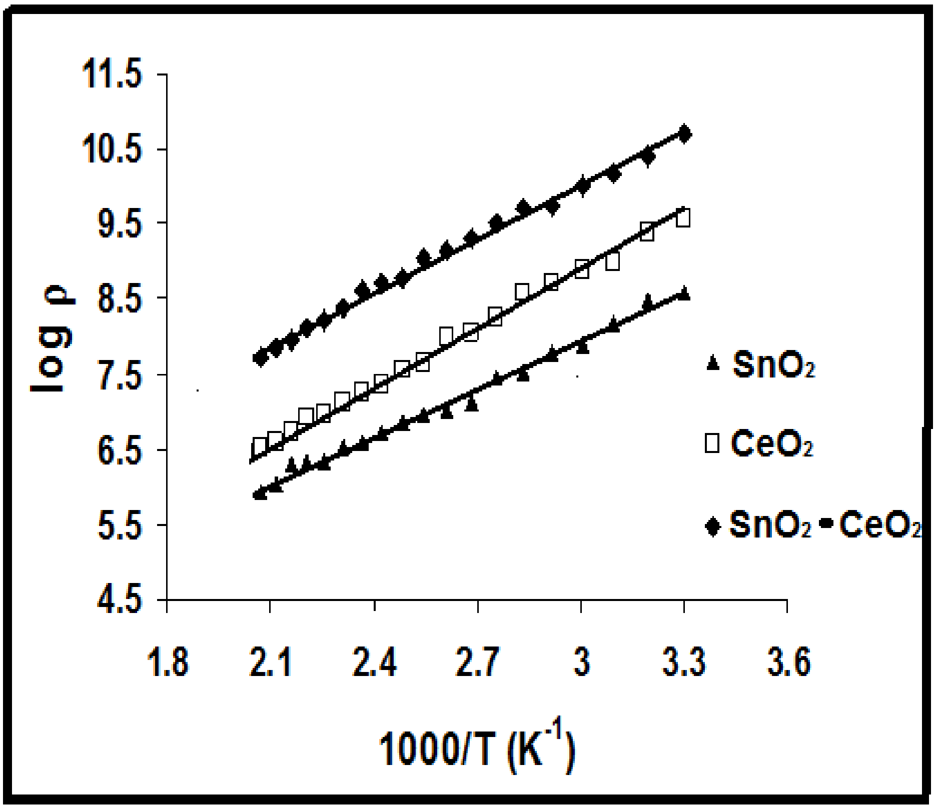

Fig. 3: Electrical resistivity study of CeO_2, SnO_2 and CeO_2-SnO_2

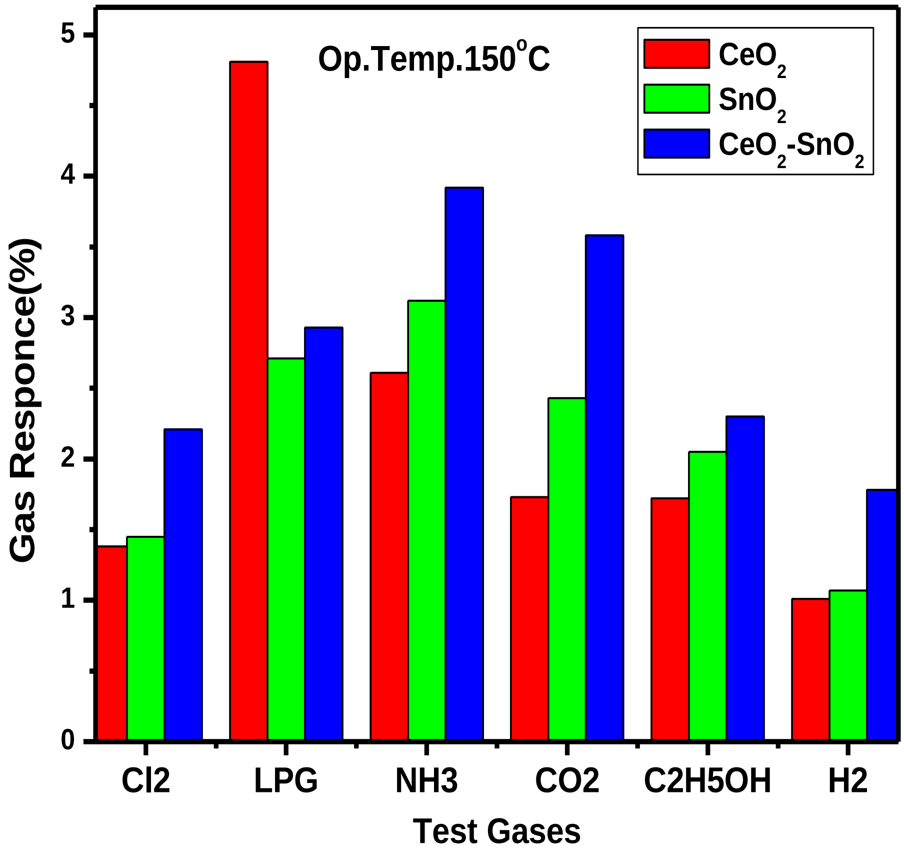

Fig. 4: Gas sening study of CeO_2, SnO_2 and CeO_2-SnO_2 Samples

Conclusion

Nanosized ceria (CeO_2), cassiterite (SnO_2) and ceria-cassiterite (CeO_2-SnO_2) nanocomposite were successfully synthesized by using microwave method. This method is cost-effective and environmentally friendly because of no by-product effluents. X-ray diffraction technique reveals that ceria (CeO_2) properly supported on the surface of cassiterite (SnO_2) and formation of single phase metal oxides. Nano sized ceria, cassiterite and ceria-cassiterite nanocomposite were confirmed by transmission electron microscopy technique. The particle size of the single oxides like CeO_2, SnO_2 and their nano composite is in the range of 10-20 nm.

The electrical resistivity is decreasing with increasing temperature for all the samples. This indicates that all the samples show semiconductor-like behavior. Various reducing and oxidizing gases were tested for gas sensing activity of all the compositions. CeO_2 shows remarkable response towards LPG with good selectivity.

Acknowledgement

Author (R.P. Patil) is thankful to Shivaji University, Kolhapur for financial assistance through minor research project under Research Initiation Scheme.

References

1. Hankare P.P., Patil R.P., Jadhav A.V., Garadkar K.M. and Sasikala R., Enhanced photocatalytic degradation of methyl red and thymol blue using titania–alumina–zinc ferrite nanocomposite, *Applied Catalysis B: Environmental,* **107**, 333–339 **(2011)**

2. Mane C.B., Khobare R.V., Patil R.P. and Pawar R.P., Photocatalytic Degradation of Methyl Red using CeO_2, TiO_2 and CeO_2-TiO_2 Nanocomposite, *International J. Applied Engineering Research*, **13**, 14372-14377 **(2018)**

3. Patil R.P., Nikam P.N., Delekar S.D., Patil D.R. and Hankare P.P., Cr-Substituted Zn–Mn Ferrospinel Thick Film Gas Sensors, *Sensor Letters*, **12**, 1–5 **(2014)**

4. Docherty C.J., Lin C.T., Joyce H.J., Nichola R.J., Herz L.M., Li L.J. and Johnston M.B., Extreme sensitivity of graphene photoconductivity to environmental gases, *Nat. Commun*., **3**, 1228 **(2012)**

5. Yan Y., Wladyka C., Fujii J. and Sockanathan S., $Prdx_4$ is a compartment-specific H_2O_2 sensor that regulates neurogenesis by controlling surface expression of GDE2, *Nat. Commun*., **6**, 7006 **(2015)**

6. Lehner P., Staudinger C., Borisov S.M. and Klimant I., Ultra-sensitive optical oxygen sensors for characterization of nearly anoxic systems, *Nat. Commun*., **5**, 4460 **(2014)**

7. Ma J., Mei L., Chen Y., Li Q., Wang T., Xu Z., Duan X. and Zheng W., Fe_2O_3 nanochains: Ammonium acetate-based ionothermal synthesis and ultrasensitive sensors for low-ppm-level H_2S gas, *Nanoscale*, **5**, 895–898 **(2013)**

8. Xu S., Gao J., Wang L., Kan K., Xie Y., Shen P., Li L. and Shi K., Role of the heterojunctions in In_2O_3-composite SnO_2 nanorod sensors and their remarkable gas-sensing performance for NO_x at room temperature, *Nanoscale*, **7**, 14643–14651 **(2015)**

9. Hoffmann M.W.G., Prades J.D., Mayrhofer L., Hernandez-Ramirez F., Järvi T.T., Moseler M., Waag A. and Shen H., Highly selective SAM-nanowire hybrid NO_2 sensor: Insight into charge transfer dynamics and alignment of frontier molecular orbitals, *Adv. Funct. Mater.*, **24**, 595–602 **(2014)**

10. Leite E.R., Weber I.T., Longo E. and Varela J.A., A new method to control particle size and particle size distribution of SnO_2 nanoparticles for gas sensor applications, *Adv. Mater.*, **12**, 965–968 **(2000)**

11. Liu J., Wang X., Peng Q. and Li Y., Vanadium pentoxide nanobelts: Highly selective and stable ethanol sensor materials, *Adv. Mater.*, **17**, 764–767 **(2005)**

12. Izu N., Hagen G., Schönauer D., Röder-Roith U. and Moos R., Application of $V_2O_5/WO_3/TiO_2$ for Resistive-Type SO_2 Sensors, *Sensors*, **11**, 2982–2991 **(2011)**

13. Weppner W., Solid-state electrochemical gas sensor, *Sens. Actuators*, **12**, 107–119 **(1987)**

14. Miura N., Nakatou M. and Zhuiykov S., Impedancemetric gas sensor based on zirconia solid electrolyte and oxide sensing electrode for detecting total NOx at high temperature, *Sens. Actuators B Chem.*, **93**, 221–228 **(2003)**

15. Kulkarni G.S., Reddy K., Zhong Z. and Fan X., Graphene nanoelectronic heterodyne sensor for rapid and sensitive vapour detection, *Nat. Commun.*, **5**, 4376 **(2014)**

16. Borini S., White R., Wei D., Astley M., Haque S., Spigone E., Harris N., Kivioja J. and Ryhanen T., Ultrafast Graphene Oxide Humidity Sensors, *ACS Nano*, **7**, 11166–11173 **(2013)**

17. Chen Z., Umar A., Wang S., Wang Y., Tian T., Shang Y., Fan Y., Qi Q., Xu D. and Jiang L., Supramolecular fabrication of multilevel graphene-based gas sensors with high NO_2 sensibility, *Nanoscale*, **7**, 10259–10266 **(2015)**

18. Lee J.S., Kwon O.S., Park S.J., Park E.Y., You S.A., Yoon H. and Jang J., Fabrication of ultrafine metal-oxide-decorated carbon nanofibers for DMMP sensor application, *ACS Nano*, **5**, 7992–8001 **(2011)**

19. Gurlo A., Nanosensors: Towards morphological control of gas sensing activity, SnO_2, In_2O_3, ZnO and WO_3 case studies, *Nanoscale*, **3**, 154–165 **(2011)**.

(Received 15th August 2020, accepted 19th October 2020)